Properties Improvement of PMMA Using Nano TiO_2

Amit Chatterjee[1,2]

[1]*Naval Material Research Laboratory, DRDO, Ambernath, India*
[2]*Center for Composite Materials, University of Delaware, Newark, Delaware*

Received 17 December 2009; Revised 18 March 2010; accepted 26 March 2010
DOI 10.1002/app.32567
Published online 30 June 2010 in Wiley InterScience (www.interscience.wiley.com).

ABSTRACT: TiO_2 nanofillers (5 nm, 0–15% weight) have been introduced in the PMMA matrix using a twin screw extruder to increase the performance of PMMA. The twin screw extrusion process is optimized to disperse the particles into PMMA. Nanofiller infusion improves the thermal, mechanical, and UV absorption properties of PMMA. TiO_2-PMMA nanocomposites exhibit the increase in tensile modulus (90%), decomposition temperature (31%), dimension stability (~ 60%) and UV absorption (~ 410%). Properties of the nanoTiO_2-PMMA composites are depending on the dispersion of TiO_2 in the PMMA matrix. It is interrelated with loading. Formation and disappearance of the peaks in FTIR confirm the chemical interaction of PMMA with TiO_2. © 2010 Wiley Periodicals, Inc. J Appl Polym Sci 118: 2890–2897, 2010

Key words: PMMA; TiO_2; nanocomposite; tensile modulus; dimension stability

INTRODUCTION

In recent years, polymer nanocomposites have received significant attention, both in the industry and academia. It represents an attractive set of inorganic–organic materials (organic–organic in some cases) and polymers at a new scale intermediate between the nano and microscale. A number of experimental investigations on these materials have indicated that the polymer nanocomposites exhibit new and sometimes improved properties that are not displayed by the individual phases or by their conventional composite counterparts.[1] Nanoparticles have extremely high surface area to volume ratios, and can alter the mobility of polymer chains near their interfaces. So, even a small addition of nanoparticles has the potential to drastically transform the properties of the host polymer. In last decade, several advancements in the field of nanocomposites have been achieved. But, some recent reviews have made it clear that the definitive structure–property relationships are still lacking in the literature.[2]

The properties of nanocomposites depend on the type of incorporated nanoparticles, their size and shape, concentration and interactions with the polymer matrix.[1–5] Various nanoparticles are incorporate into the polymer matrix for nanocomposite applications. Among them, nanocomposite with nanoscaled TiO_2 embedded has gained great interests to scientists and researchers around the world because of the unique properties.[6] Various polymer/TiO_2 nanocomposites were prepared by the sol-gel process for different purposes.[1,2] A series of nanocomposites with high refractive index, incorporating the TiO_2 colloids into several polymers, with improve optical and electrical properties were reported as well.[7–9] Solar cells, based on the nanocomposites of polymers with TiO_2 showed some excellent photovoltaic cell efficiency.[7–11] Even when, TiO_2 was simply used as the filler for the coatings, plastics, and rubbers, the resultant nanocomposites showed improved performance in UV-shielding,[12] dynamic fracture toughness, flame retardant, optical transparency, scratch resistance, and chemical resistance.[2,12–14] Most of the TiO_2-composites are based on various types of resins matrix. PMMA is an interesting polymer for mechanical and optical applications[10] due to its easy possibility and high transparency in the visible range. The PMMA-TiO_2 nanocomposites are counting in number. PMMA-TiO_2 composites are used as additives, ultra fast optical nonlinearity measurements, optical waveguide, photovoltaic application, semiconductor materials and for biomedical applications.[9,15–20] The majority of them are practically used to enhance the optical and dielectric stability. Very few are demonstrated the mechanical performance improvements, and they are mainly in-site-to polymerization of MMA in presence of TiO_2. Even sol-gel method was used for TiO_2 formation in the polymerization process of MMA to PMMA. Recently, surface modified TiO_2 was dispersed in PMMA to improve the performance of PMMA.[2] It is reported that the surface unmodified TiO_2 decreases T_g and other mechanical properties of PMMA.[2] Information

Correspondence to: A. Chatterjee (Chatterjeamit@yahoo.com).

are limited for the straight forward mixing of unmodified TiO_2 (5 nm) in PMMA matrix to improve the thermal and mechanical properties of host polymers. In our earlier publication[16] we have mixed TiO_2 in the thermoset system, and have achieved the properties improvement for the epoxy matrix.

In this research, TiO_2 is directly mixed with PMMA polymer in a twin screw extruder machine. The UV absorption, dimension stability, mechanical, and thermal properties in air of the nanocomposites were studied. The chemical interaction of the TiO_2 nanoparticles on PMMA has been investigated using FTIR. Reasons for the improvement of properties have been explained.

EXPERIMENTAL

Materials and methods

The TiO_2 nanoparticles of 5 nm size were supplied by Nanostructured and Amorphous Materials INC, Los Alamos, NM. Properties of the particles were reported, previously.[16] PMMA was purchased from Scientific Polymer Products (Ontario, NY). The density (g/cc) at (25°C), refractive index, inherent viscosity, F_p, T_g and polydispersity (PDI) of PMMA are 1.20, 1.490, 1.25, 572, 95, and 2.8, respectively.

Preparation of thin film polymer-titanium composites using extrusion processing

Required amount of PMMA and TiO_2 by weight, were mixed in a beaker. The mixture was stirred for 12 min using a wooden stick. The DACA twin screw extruder, DACA Instruments, Santa Barbara, CA 93,101, was turned on and heated to 190°C. The extruder screws were set to turn at a rate of 100 rpm. The PMMA-TiO_2 mixture was placed into the extruder injector. Sample was allowed to mix in the machine for 7 min and then extruded out. The extracted samples were cut into small pieces, reinjected into the machine and let to mix for another 8 min. This was repeated several times to get uniform mixture. The hot press was heated at 190°C. Two flat aluminum plates were cleaned using acetone and then a layer of frekote was applied. When the hot press's was reached at 190°C the extruded sample was placed onto the aluminum plates. Two long aluminum blocks were placed beside the aluminum plates onto the hot press for controlling the pressure and heating uniformity. 30 min optimum time was used to heat up, and melt the samples in the press. The long metal blocks were then removed, and hot press was closed. A pressure of 35 tons was applied to press the samples. The hot press was left in the clamping position for 30 min. The heat was turned off, and the cooling system was turned on while the plates were still remained clamped. The plates were removed when the temperature of the hot press was reached below 40°C. The film was removed from the plates. A razor blade was used to cut the film into various sizes for analysis. More details about the preparation procedure have been described previously.[20]

Characterization techniques

Dynamic mechanical analysis was conducted (DMA 2980) at a frequency of 1 Hz using a Film Tension Clamp. The force ramp experiment was used to get the stress strain data and to determine the linear viscoelastic region for the samples. The samples were ramped from 1 N/min to 18 N. The stress–strain curves were generated. The modulus was measured from the slope. The nanocomposite thin films samples were cut into rectangular shapes $10.0 \times 6.0 \times 0.3$ mm^3 for DMA analysis. Dimension stability was measured from the DMA experiment.

Thermogravimetric analysis

Thermogravimetric analysis (TGA Q-500, TA) was used to measure the degradation properties of the nanocomposites. The experimental parameters are: heating rate of 10°C/min, room temperature to 900°C, flow rate of nitrogen and air is 90 + 10 mL/min. The EGA furnace was used for the experiment. The air was used for oxidative study.

Spectroscopy

FTIR analysis of the samples was carried out using a Nicolet MAGNA-IR 860 spectrometer with DTGS detector. Dry nitrogen gas was purged all the time to the sample compartment to remove the water and CO_2 interference from air. The thin films samples were placed in a sample holder and wait for 10 min before the FTIR spectrum was taken. The spectra were recorded from 400 to 4000 cm^{-1} at a resolution 1 cm^{-1} for 400 scan. The gain on the instrument was set to 1.0. UV–vis spectra were measured on a Perkin–Elmer Lambda 35 UV–vis spectrometer at the wavelength range 190–400 nm. Scanning electron microscopy was conducted in JXA-840 scanning electron microscope. The samples were gold coated before analysis. The filament voltage was set at 10–30 KV to make an image of the nanostructure.

DSC

DSC-Q100 from TA instrument was used to characterize the total heat of reaction, and T_g. For the DSC experiments, 5 mg of samples were taken into the DSC pan. The sample was ramped from −90 to

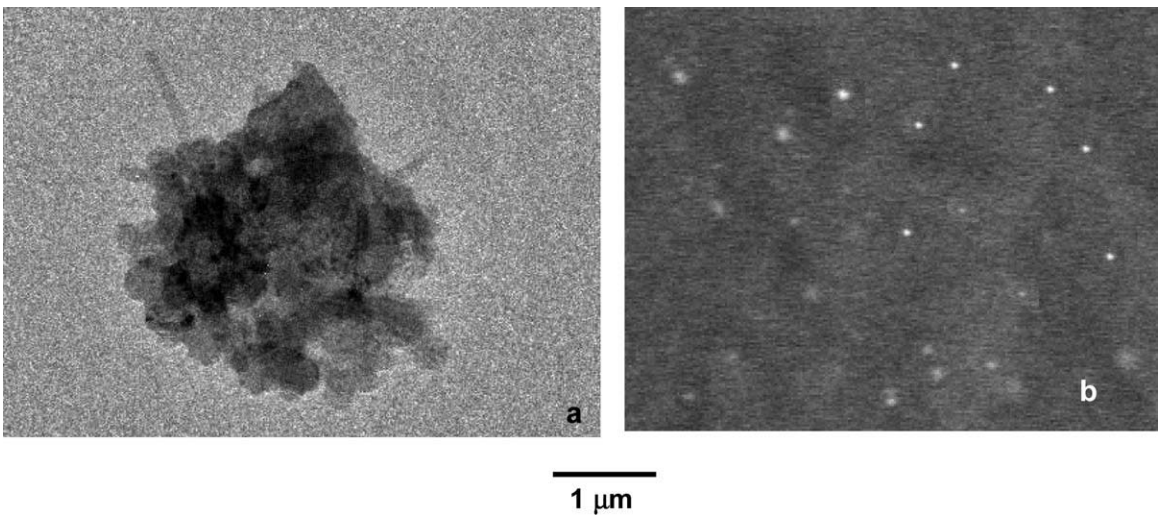

Figure 1 SEM images of (a) 5 nm powder TiO_2 and (b) 2% by wt TiO_2-PMMA-nanocomposites; five times extruded.

300°C at a constant rate (10°C/min). The heating and cooling were repeated to get the transition characteristic. The T_g was measured from the phase change.

RESULTS AND DISCUSSION

Dispersion of nanoparticles

Nanoparticles dispersion in the PMMA resin is difficult because of the Van der Waal's force between the nano TiO_2 particles. Scanning electron microscopy (SEM) analysis was conducted to verify the dispersion quality of the nanocomposite. We have seen previously that the TiO_2 nanoparticles before adding to the PMMA are agglomerated highly.[16] Figure 1(a,b) shows the SEM images for 5 nm powder TiO_2 particles and 2% TiO_2-PMMA nanocomposite (five times extruded). The nano particles are agglomerated [Fig. 1(a)]. The lumps of TiO_2 particles are found in the single time extruded TiO_2-PMMA nanocomposite sample. However, most of the particles are distributed uniformly after five times extrusion [Fig. 1(b)]. Efforts are continuing to focus on improving more homogenous dispersion of the TiO_2 nanoparticle with increasing the extrusion times.

Mechanical and viscoelastic performance

The dynamical mechanical tests are conducted at room temperature to see the physical, chemical, and structural changes of the polymers and the nanocomposites. The stress–strain curves are presented in Figure 2. In Table I, modulus at 25°C, are reported. Tensile modulus for all the composites containing fillers is pushed to a higher level relative to that of the neat resin system. The variation of modulus as a function of TiO_2 content is shown in Table I. Modulus of the nanocomposite has been increased with increasing the weight of the TiO_2 content. At 25°C, for 15% TiO_2-PMMA nanocomposite, tensile modulus has been increased about 95% compared to that of the virgin PMMA (Table I). T_g (DSC curves) for the TiO_2-PMMA nanocomposites increased, 23% with the TiO_2 nanoparticle addition, Table I. The dimension change is decreased with the nanoparticles addition, as shown in Figure 3. So, TiO_2 has increased the dimensional stability of the TiO_2-PMMA nanocomposite for more than 60%. In general, modulus increases monotonically with the addition of TiO_2. However, the rate of the increase of modulus, T_g, and dimensional stability are greater at the lower volume fractions. The absolute values of modulus were higher for nanocomposites fabricated using higher mass. The overall increase in modulus, dimensional stability and T_g are significant, especially for the materials processed at the lower concentration of nano TiO_2. At 2% TiO_2 addition, modulus is 34% higher; T_g is 20% higher than

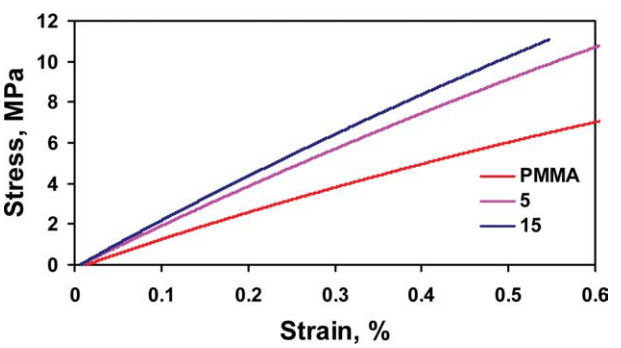

Figure 2 Stress–strain graph for pure PMMA and TiO_2-PMMA-nanocomposites. [Color figure can be viewed in the online issue, which is available at www.interscience.wiley.com.]

TABLE I
Thermal (Decomposition Temperatures, Temperature of Maximum Rate of Weight Loss, Char Content) and Mechanical Performance (% Increased) for PMMA and NanoTiO_2-PMMA-Nanocomposites

wt % of TiO_2	Temperature, °C at % weight loss started				Residue, %	Max. Decom. Temp., °C	T_g, °C, (DSC)	% T_g Inc.	Ten. Mod. (MPa)	% Ten. Mod. Inc.
	1%	5%	50%	90%						
0	167	217	343	380	0.9	346	104	0	1201	0
5	205	313.6	369	394	5.6	378	123	18	1905	59
15	173	310	376	411	11.2	384	128	23	2340	95

that of the virgin PMMA. These improvements in properties are significant for the nominal use of nano TiO_2 (2% wt). The TiO_2-PMMA nanocomposites behave like the two-phase composites with spheroids having lower aspect ratio. Because of the high modulus of TiO_2 and the improved interfacial adhesion between nanoparticles and PMMA,[18] mechanical load imposed on the nanocomposites is transferred through the interfacial surface to the strongest nanoparticles efficiently. Therefore, the mechanical performance of the nanocomposite has been improved.

In most of the cases, crosslink density is the key factor for controlling T_g, modulus and dimensional stability for the polymer system. In the present study, improved modulus, dimensional stability and T_g for the TiO_2-PMMA nanocomposite indicates that TiO_2 has chemically and physically interacted with PMMA. The TiO_2 can react with —COOR group of PMMA polymer in two different ways. One way is in the form of H-bond between carbonyl group and surface hydroxyl group of TiO_2. Another way is that TiO_2 might be bound with two oxygen atoms of —COOR by a bidentate coordination to Ti^{4+} cation.[18,19] As a result, when TiO_2 comes to the surface of the polymer PMMA it might form the crosslink structure and bound to the PMMA. This bonding increases with increasing TiO_2 loading as number of particles increases with loading. TiO_2 generally synthesized through sol-gel method from Ti-compounds. The existence of the surface —OH is most probable and this is confirmed by the FTIR at 3100–3500 cm^{-1}. Many research articles have confirmed the presence of surface hydroxyl group in TiO_2. Therefore, the hydrogen bonding between the —OH group of TiO_2 and the C=O group of methyacralate is taking place. The Ti—O—C bonds through crosslinking between TiO_2 and PMMA is feasible, and has been confirmed by FTIR that will be discussed in the later section. The improved in modulus value with the increment of nano TiO_2 concentration has been further confirmed the chemical linkage of TiO_2 and PMMA that enhances the crosslink density of TiO_2-PMMA. The enhancement in T_g may be attributed to a loss in the mobility of chain segments of the PMMA system. Impeded chain mobility is possible if the nanoparticles are well dispersed in the matrix. The particle surface-to-surface distance should be relatively small and chain segment movement is restricted. The good adhesion of nanoparticles with the surrounding polymer matrix would be the additional benefit to get better dynamic modulus by hindering the molecular motion. Moreover, the hard particles incorporated into the polymer would act as the virtual network nodes that also help for the enhancement of T_g, dimensional stability and modulus.

Thermo-oxidative study of nanoTiO_2-PMMA composite in air

The thermal decomposition experiments of PMMA and PMMA-TiO_2 nanocomposites were performed in air (Fig. 4). DTA curve of pure PMMA shows two peaks (205 and 346°C). First peak corresponds to depolymerization initiated by the saturated chain ends whereas the second peak represents the depolymerization started by the random main chain scission. The mechanism of thermo-oxidative degradation of PMMA in air is much more complex than the mechanism of degradation in nitrogen. Oxygen suppresses the degradation caused by the presence of the weak linkages in the PMMA chains at the low temperature, but it enhances the PMMA degradation at higher temperature,[17] as shown in Figure 4. The second DTA peak, which appears very broad, may

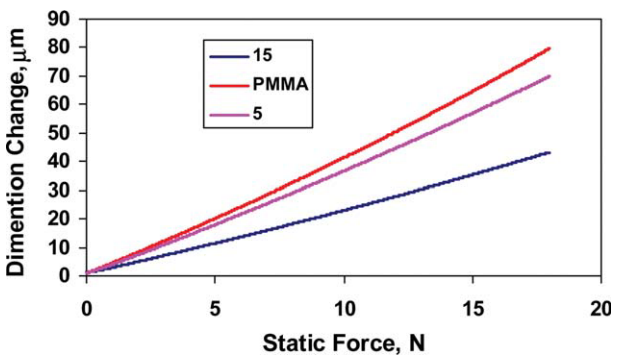

Figure 3 Dimension change graphs for pure PMMA and TiO_2-PMMA-nanocomposites. [Color figure can be viewed in the online issue, which is available at www.interscience.wiley.com.]

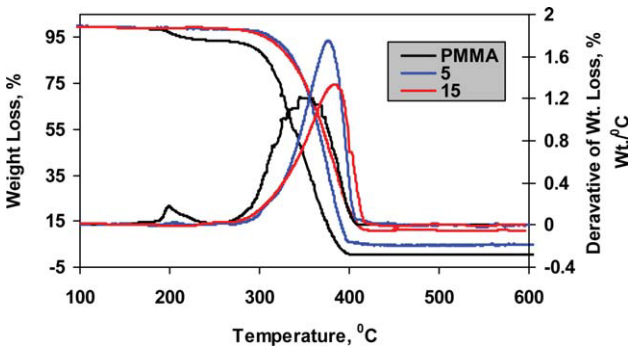

Figure 4 Thermal decomposition profile in air (TGA and DTA graphs) for pure PMMA and TiO_2-PMMA-nanocomposites. [Color figure can be viewed in the online issue, which is available at www.interscience.wiley.com.]

be the sum of two overlapped peaks. Those peaks correspond to the degradation of the PMMA matrix. The peak temperature is shifted to a higher temperature with increasing the content of TiO_2 in the nanocomposite. The DTA peak of pure PMMA is at 346°C, and that for the PMMA-TiO_2 nanocomposite sample is at about 380°C. The inhibiting effect of the TiO_2 particles increases the peak temperatures for the nanocomposites. Two types of reactions are happening between oxygen and TiO_2. The first type of reaction occurs on the materials surface. It is related to the exchange of free electrons from the material with the adsorbed gas. The second type of reaction occurs in the bulk of the material. It is represented by the exchange of oxygen ions from the gas with oxygen vacancies in the materials. The surface reaction usually occurs at lower temperatures (300–500°C), while the bulk reaction takes place at higher temperatures (700–900°C). Anatase TiO_2 crystalline phase has more free electrons than rutile phase and that can be associated to surface reactions. Oxygen that diffused in the nanocomposite samples was absorbed on the surface of TiO_2. Hence, diffuse oxygen amount in the PMMA matrix was lower than in pure PMMA, which led to the slower thermo-oxidative degradation of the PMMA matrix.[20] The broad peak for nanocomposite is observed. This phenomenon reveals that the incorporation of TiO_2 into the networks of PMMA would promote the thermal stability of hybrids. Owing to the low surface energy of TiO_2, it would result in migration to the surface of resins to form a heat-resistant layer. The thermal stability of the nanocomposite increases with nano TiO_2 loading. The 5% weight loss for the neat PMMA and TiO_2-PMMA-nanocomposite are occurred at 217 and 310°C respectively, as seen in Figure 4, Table I. Researchers are commonly considered 50% weight loss as an indicator for structural destabilization.[21] So, in the present study 50% of the total weight loss is considered as the structural destabilization point of the system. It is clearly observed that the neat resin sample without TiO_2 nanoparticles is stable up to 167°C (1% weight loss), where as with 5% TiO_2 loading the composite is stable up to 205°C, as observed in Table I. Generally, polymer having higher crosslink density shows higher maximum decomposition temperature.[22] The Increment of decomposition temperature with TiO_2 loading is due to the barrier formation of heat and oxygen in the PMMA matrix by the ceramic nature of TiO_2 particles.

Chemical interaction study

Fourier transform infrared (FTIR) spectroscopy was used to investigate the nature of the chemical interaction of PMMA on TiO_2. FTIR results are presented in Figures 5–8. The carbonyl groups at 1720 cm^{-1} is present for all the samples including PMMA. The new peaks at 1643 and 2920 cm^{-1} are appeared in nanocomposites, Figures 5–7. These peaks are missing in pure PMMA. The disappearance and generation of new peaks for the nanocomposite indicate the chemical interaction between the PMMA and TiO_2. The broad bands at the range of 400–700 cm^{-1} are evidence for Ti—O—Ti network structures.[23] Peak at 483 cm^{-1} for PMMA is shifted to lower side with nano-addition. The peak area increases with TiO_2 addition. The peak intensity 748 cm^{-1} decreases with TiO_2 increment. Two bands 2920 cm^{-1} and 2992 cm^{-1} are appearing due to —CH_2 stretching modes of PMMA, Figure 7. The asymmetric stretching mode at 2992 cm^{-1} shows no change in its position while the intensity varies with filler content. It decreases with nano TiO_2 addition. The symmetric stretching mode at 2920 cm^{-1} exhibits noticeable changes in position as well as intensity for the nanocomposites. The peak at 2920 cm^{-1} is lacking in pure PMMA, as seen in Figure 7. These changes are the indication of the PMMA's interactive role with fillers. The 2948 cm^{-1} peak for the TiO_2-PMMA-nanocomposite decreases with the enhancement of TiO_2 content (0–15%) and the 2920 cm^{-1} peak intensity become more intense with nano addition. The (—CH_3) group asymmetric deformation vibration is occurred at 1433 and 1480 cm^{-1} for PMMA, whereas the (—CH_3) symmetric vibration is centered at 1386 cm^{-1} for all the nanocomposites. Characteristic absorptions due to the stretching of ether (C—O) carbon and carbonyl (C=O) of the ester group are observed at 1140 and 1720 cm^{-1} for all the composites, respectively. The peaks are flattened with nano addition. It indicates that C—O and C=O are bonding with TiO_2, and that helps for the peak flattening and shifting. This is due to the coordination of Ti^{+4} with carbonyl oxygen on the ester side of PMMA that is acting as a transient crosslinks.[18]

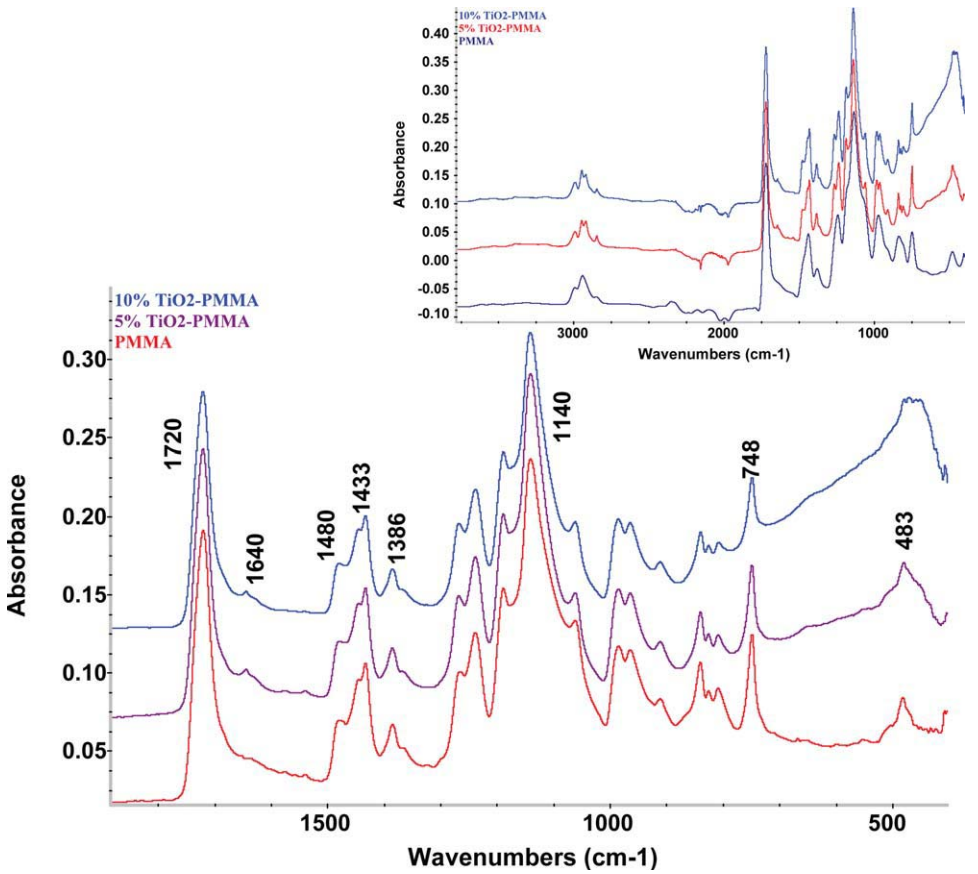

Figure 5 FTIR Spectra for pure PMMA and TiO_2-PMMA-nanocomposites; inset: Complete spectral range from 400–3700 cm^{-1}. [Color figure can be viewed in the online issue, which is available at www.interscience.wiley.com.]

The broad spectrum in the range of 3500–3100 cm^{-1} is observed for the TiO_2-PMMA-nanocomposites (Fig. 8). Two peaks at 3391 and 3191 cm^{-1} are found for nanocomposite samples (Fig. 8). This can be attributed to the hydroxyl and hydroperoxide stretching vibration that is induced due to the attack of —OH and the subsequent formation of polymer peroxy link with TiO_2. However, pure PMMA sample did not shows the —OH peak. Below 2000 cm^{-1}, the spectra for the TiO_2 nanocomposites show two characteristic bands at 1480 and 1433 cm^{-1} respectively. These vibration bands are related with the —$COOCH_3$ antisymmetric vibration and the symmetric stretching vibration of acrylate anions complexes with surface Ti centers. The evidence for the free C=O stretching band at around 1640–1720 cm^{-1} seems the C=O involvement in the H-bonding with a Ti—OH surface group. The FTIR analysis clearly

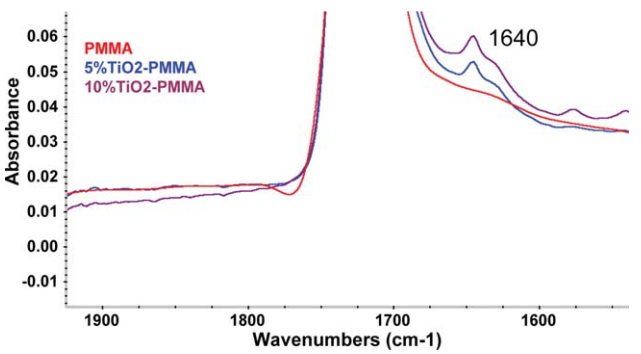

Figure 6 FTIR Spectra for pure PMMA and TiO_2-PMMA-nanocomposites in the spectral range 1500–2000 cm^{-1}. [Color figure can be viewed in the online issue, which is available at www.interscience.wiley.com.]

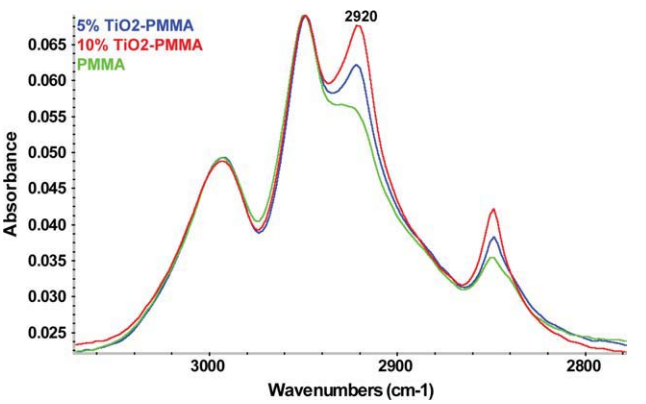

Figure 7 FTIR Spectra for pure PMMA and TiO_2-PMMA-nanocomposites in the spectral range 2800–3100 cm^{-1}. [Color figure can be viewed in the online issue, which is available at www.interscience.wiley.com.]

shows the coordination behavior of the polar moiety of the $-COOCH_3$ bonding with the TiO_2 surface atoms. The sample compartment of the FTIR machine is always saturated with N_2 gas before acquiring the FTIR measurement. The FTIR spectra are background corrected. So, CO_2 interference from the air has been automatically corrected. The main peak for the CO_2 in FTIR (100% intensity) is at 2340–2360 cm^{-1} range. However, no peak is found in that spectral range for all measured samples (Fig. 5 inset). So, the CO_2 interference is less likely. Increasing the nanoTiO_2 concentration the peak intensity at 2920 cm^{-1} has been amplified (Fig. 7) that clearly shows that the peak is from TiO_2 interaction with PMMA. If the peak at 2920 cm^{-1} is appeared from air CO_2, the peak intensity (height/area) will remain same for all the measured samples.

UV-absorption characteristic

The spectra of the TiO_2-PMMA-nanocomposites (2–15%) were taken with increasing the TiO_2 concentration (2–15%). All the UV spectra are alike and reached the maximum limit of UV absorption at 2% TiO_2 concentration. There is no change in UV absorption property (intensity) between 2 and 15% nanoTiO_2 additions. So, 2% of TiO_2 nanofillers reached the critical amount to UV properties. Figure 9 shows the UV spectra of pristine TiO_2 and 2% TiO_2-PMMA composites. The pristine TiO_2 nanoparticles exhibited a strong UV absorption at 320 nm, assigned to the typical absorption edge of TiO_2.[24] Upon modification of PMMA with nano TiO_2, maximum peak of UV absorption is blue-shifted to 283 nm, indicating the successful interaction of PMMA with TiO_2. In the spectral range of 400–300 nm the 410% improvement of UV absorption is occurred in the TiO_2-nanocomposite compared to PMMA. These results of UV absorption demonstrate the presence of the chemical interaction of PMMA on the TiO_2 surface. They are successful interacted with each other. The prepared composite films are transparent. The onset of UV absorption for the nanocomposites is as a result of the excitation of electrons from the valence band to the conduction band of titania.[25] The UV shielding property of the nanocomposites can be easily controlled by adjusting the inorganic content in the PMMA matrix while the transparency in visible region can still be maintained. Because the Titania particles are in nanometer-scale and are well dispersed in PMMA matrix.

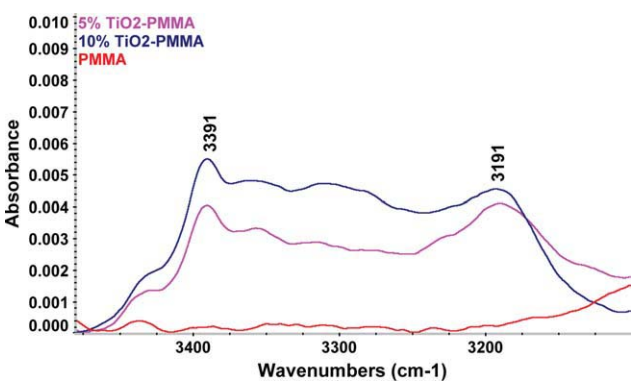

Figure 8 FTIR Spectra for pure PMMA and TiO_2-PMMA-nanocomposites in the spectral range 3100–3500 cm^{-1}. [Color figure can be viewed in the online issue, which is available at www.interscience.wiley.com.]

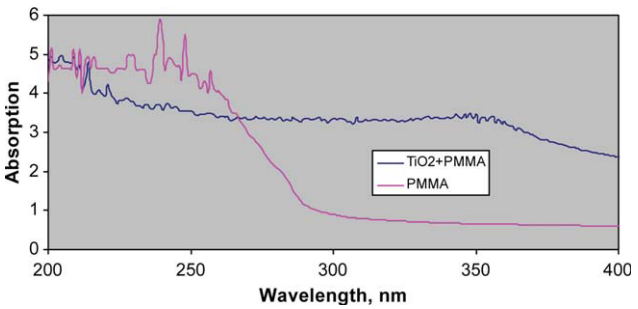

Figure 9 UV absorption characteristic properties of PMMA and TiO_2-PMMA–nanocomposites. [Color figure can be viewed in the online issue, which is available at www.interscience.wiley.com.]

CONCLUSION

The nanoTiO_2-PMMA nanocomposites were prepared by mixing various weight percent of TiO_2. The incorporation of TiO_2 improves the thermal, dimensional stability, UV absorption, mechanical properties and T_g of PMMA. The tensile modulus was improved by 90%, and UV absorption by 410% with the addition of nano TiO_2. The presence of TiO_2 leads the improvement in properties due to the chemical interaction of PMMA with TiO_2. The FTIR and UV characterizations evidence for the chemical interaction of TiO_2 with PMMA. The chemical and physical interactions improve the performance of the nanocomposites. The thermal stability is improved due to heat inhibiting effects of the TiO_2 particles in the degradation stages of PMMA. PMMA has numerous applications starting as medical, biomedical to common structural and transparent materials. Nano TiO_2 can be used for the property improvement of PMMA with minimum loading as low as 2%.

References

1. Tanniru, M.; Yuan, Q.; Misra, R. D. K. Polymer 2006, 47, 2133.
2. Lesley, M.; Hamming, L. M.; Rui Qiao, A. B.; Phillip, B.; Messersmith, A. C.; Brinson, L. C. Comp Sci Technol 2009, 69, 1880.
3. Yuwono, A. H.; Liu, B.; Xue, J.; Wang, J.; Elim, H. I.; Ji, W. J Mater Chem 2004, 14, 2978.

4. Lu, S. R.; Zhang, H. L.; Zhao, C. X.; Wang, X. Y. Polymer 2005, 46, 10484.
5. Pandey, J. K.; Reddy, K. R.; Kumar, A. P.; Singh, A. P. Polym Degrad Stab 2005, 88, 234.
6. Li, F.; Zhou, S.; You, B.; Wu, L. J Appl Polym Sci 2006, 99, 3281.
7. Kubacka, A.; Serrano, C.; Ferrer, M.; Lunsdorf, H.; Bielecki, P.; Cerrada, M. L. Nano Lett 2007, 7, 2529.
8. Haggenmueller, R.; Gommans, H. H.; Rinzler, A. G.; Fischer, J. E.; Winey, K. I. Chem Phy Lett 2000, 330, 219.
9. Chatterjee, S.; Chatterjee, A. Jpn J Appl Phys 2008, 47, 1136.
10. Hornak, H. A. Polymers for Lightwave and Integrated Optics; Marcel Dekker: New York, 1992.
11. Wakabayashi, K.; Pierre, C.; Dikin, D. A.; Ruoff, R. S.; Ramanathan, T.; Brinson, T. C. Macromolecules 2008, 41, 1905.
12. Qiao, Q. Q.; Xie, Y.; Mcleskey, J. T. J Phys Chem C 2008, 112, 9912.
13. Dridi, C.; Barlier, V.; Chaabane, H.; Davenas, J.; Ben Ouada, H. Nanotechnology 2008, 19, 11.
14. Yang, C. C.; Chiu, S. J.; Lee, K. T.; Chien, W. C.; Lin, C. T.; Huang, C. A. J Power Source 2008, 184, 44.
15. Pen, J.; Vallet-Regí, M.; San Roman, J. J Biomed Mater Res 1997, 35, 129.
16. Chatterjee, A.; Islam, M. S. Mat Sci Eng A 2008, 487, 574.
17. Kwak, G. H.; Park, S. J.; Lee, J. R. J Appl Polym Sci 2000, 78, 290.
18. Annalisa Convertino, A.; Gabriella Leo, A.; Marinella Striccoli, B.; Gaetano Di Marco, C.; Lucia Currib, M. Polymer 2008, 49, 5526.
19. Handa, M.; Tojo, M.; Osawa, T. Eur Pat Appl 1998, EP0879695, 21.
20. Chatterjee, A. J Appl Polym Sci 2010, 116, 3396.
21. Mathew, A. P.; Packirisamy, S.; Thoms, S. Polym Degrad Stab 2001, 72, 423.
22. Horowitz, H. H.; Metzger, G. Anal Chem 1963, 35, 1464.
23. Rajh, T.; Nedeljkovic, J. M.; Chen, L. X.; Poluektov, O.; Thurnauer, M. C. J Phys Chem B 1999, 103, 3515.
24. Mbhele, Z. H.; Salemane, M. G.; Van Sittert, C. G. C. E.; Nedeljkovic, J. M.; Djokovic, V.; Luyt, A. S. Chem Mater 2003, 15, 5019.
25. Wang, H.; Xu, P.; Meng, S.; Zhong, W.; Du, W.; Du, Q. Polym Degrad Stab 2006, 91, 1455.